RESEARCH ON CURVED PATH-TRACKING CONTROLLER OF RICE TRANSPLANTER BASED ON H-INFINITY STATE FEEDBACK CONTROL
/
基于 H 无穷状态反馈控制的插秧机曲线路径跟踪控制器研究

Yueqi MA[1, 2)], Ruijuan CHI[*1, 2)], Yantao ZHAO[1, 2)], Chao BAN[1, 2], Tong SU[1, 2)], Zhengrong LI[1, 2)]
[1)] College of Engineering, China Agricultural University, Beijing 100083, China
[2)] Vehicle Intelligent Control Laboratory, China Agricultural University, Beijing 100083, China
[*]Corresponding authors. Email: chiruijuan@cau.edu.cn
DOI: https://doi.org/10.35633/inmateh-73-41

Keywords: *Unmanned transplanter; Path-tracking; H-infinity control; Linear matrix inequality*

ABSTRACT
The accuracy of curved path-tracking for headland turning of transplanters is crucial to maintaining the row spacing precision required for rice planting. To address this issue, a method based on H-infinity state feedback control is proposed. In this method, the requirement of robustness is transformed into linear matrix inequalities (LMIs) to optimize the gain coefficients of the control law. The simulation test show that this method outperforms the Linear Quadratic Regulator (LQR) when facing uncertain parameters (longitudinal speed and cornering stiffness) and path curvature disturbance. In addition, the field test results show that when the transplanter tracks a 1/4 circular arc path with a radius of 2 meters, the mean value of the absolute lateral error and the absolute heading angle error using this controller are 0.029 m and 3.69°, respectively. The maximum absolute lateral error is 0.072 m, and 64% of the absolute lateral error are less than 0.04 m, meeting practical requirements. Compared with the LQR controller with feed forward control, the mean value of the absolute lateral error is reduced by 36%. This method meets the accuracy and robustness requirements for unmanned rice transplanter turning at the headland.

摘要
水稻插秧机地头转向时的曲线路径跟踪效果影响着水稻插秧机每行作业前期水稻插植的行距精度。为了提高无人插秧机曲线路径跟踪的鲁棒性，保证水田复杂环境下插秧机地头转向的精度，提出了一种基于 H 无穷状态反馈控制的插秧机曲线路径跟踪控制器设计方法。该方法将控制器对于不确定参数（纵向速度、轮胎侧偏刚度）和扰动项（路径曲率扰动）的鲁棒性需求转化为线性矩阵不等式（Linear Matrix Inequality，LMI）的形式，并以此为约束求解最优控制律增益系数,实现控制器对于不确定参数和扰动项的鲁棒性。仿真试验结果表明，该方法在系统存在不确定参数和扰动项时，相较线性二次调节器（Linear Quadratic Regulator，LQR）具有更好的路径跟踪效果。田间试验结果表明，插秧机在跟踪半径为 2m 的 1/4 圆弧路径时，该控制器控制下的曲线路径跟踪的横向偏差绝对值均值和航向角偏差绝对值均值分别为 0.029m、3.69°，横向偏差绝对值的最大值为 0.072m，绝对值小于 0.04m 的横向偏差占 64%，满足实际需求。相较于前馈 LQR 控制器，横向偏差绝对值均值降低 36%。该方法满足插秧机地头转向时曲线路径跟踪的精度与鲁棒性需求。

INTRODUCTION
Path-tracking control technology is the key to improving the accuracy and efficiency of unmanned agricultural machinery operations. Unmanned rice transplanters are a typical representative of unmanned agricultural machinery, and improving the accuracy of rice planting through path-tracking control is an inevitable requirement for precision agriculture. Currently, the straight-line path-tracking accuracy of unmanned rice transplanters has basically met the requirements, while the curved path-tracking accuracy still needs to be improved. The accuracy of curved path-tracking during the headland turning of the rice transplanter affects the row spacing precision of rice planting in the early stage of each row operation *(Li et al., 2023; Gang et al., 2022).* Therefore, the research on curved path-tracking control of rice transplanters is of great significance for improving the operational precision of unmanned rice transplanters.

The main algorithms applied in agricultural machinery path-tracking control include PID algorithm *(Gökçe et al., 2021)*, fuzzy control *(Dekhterman et al., 2024)*, pure pursuit algorithm *(Li et al., 2018)*, LQR algorithm *(Hossain et al., 2022)*, MPC algorithm *(Simonelli et al., 2023)*, and sliding mode control (SMC) *(Ji et al., 2023).*

All authors' names and titles: Yueqi MA, Ph.D. candidate; Ruijuan CHI, Associate Professor; Yantao ZHAO, Master's candidate; Chao BAN, Ph.D. candidate; Tong SU, Master's candidate; Zhengrong LI, Master's candidate.

In terms of straight-line path-tracking control, *Tang et al (2018)* improved the adaptability of straight-line path-tracking of rice transplanters to vehicle speed under pure tracking algorithm control. *He et al (2022)* and *Chi et al (2022)* applied the MPC algorithm to the straight-line path-tracking of rice transplanters and achieved optimal results. To date, the accuracy of straight-line path-tracking control for agricultural machinery and even rice transplanters has met the requirements. However, because the curvature of the expected path is not considered in the design of the straight-line path-tracking controller, the adaptability of the above methods to curved path-tracking is poor. They are not suitable for being directly applied to curved path-tracking.

Li et al (2018) improved the accuracy of rice transplanter curved path-tracking by adjusting the look-ahead distance of the pure pursuit algorithm based on vehicle speed and path curvature. They also introduced a coefficient to multiply the desired front wheel angle when the lateral error exceeds a certain threshold, enabling the controller to simultaneously control lateral error and heading angle error. However, this approach does not guarantee the optimal response of the pure pursuit controller to lateral error. Based on the pure pursuit algorithm, *Yang et al (2022)* proposed a path-tracking algorithm based on the optimal target point for agricultural machinery. The curve tracking error was reduced by more than 20% compared to the pure pursuit algorithm. Although the above methods have improved the adaptability of the path-tracking controller to path curvature, the controller design is all based on the vehicle kinematic model. This kind of model does not consider the path curvature factors and has weak adaptability to curved path-tracking *(Gong, et al., 2014)*. There are also designed curved path-tracking controllers for vehicles based on vehicle kinematic tracking error models that include expected path curvature factors. For example, based on the vehicle kinematic tracking error model, *Oh and SEO (2023)* proposed an adaptive control and sliding mode control based curved path-tracking algorithm, which further enhances the adaptability of autonomous vehicles to uncertain parameters based on pure sliding mode control. *Kim et al (2023)* calculated the tracking error based on image information and compared the path-tracking control accuracy of LQR and traditional sliding mode control based on the vehicle kinematic tracking error model. The experimental results showed that LQR was better than traditional sliding mode control. *Taghia et al (2017)* used a sliding mode controller with disturbance observer to control the path-tracking of tractors based on the vehicle kinematic tracking error model. However, the vehicle kinematic tracking error model ignores the lateral speed. When the rice transplanter performs large curvature headland turning in paddy fields, the lateral speed is relatively high. Therefore, the above method is also difficult to adapt to the curved path-tracking of the rice transplanter headland turning.

The establishment of the tracking error model based on the two-degree-of-freedom vehicle dynamics simultaneously considers path curvature and lateral speed. Therefore, this paper adopts the tracking error model based on the two-degree-of-freedom (Two-DOF) vehicle dynamics to design the curved path-tracking controller for the transplanter. There are three main types of interference in the system after the linearization of the tracking error model based on Two-DOF vehicle dynamics: the path curvature disturbance caused by the curved path, the longitudinal speed uncertainty and the cornering stiffness uncertainty caused by the complex dynamic paddy field environment. Combined with robust control *(Su, 2010)*, the design of the path-tracking controller can improve the robustness of the controller and reduce the influence of the above factors on the control accuracy.

Currently, methods for enhancing the robustness of path-tracking controllers for agricultural machinery often involve supplementing traditional algorithms such as PID and pure pursuit with fuzzy control *(Tang et al., 2018)*, neural networks *(Shojaei and Taghavifar, 2022)*, optimization algorithms such as PSO *(Gökçe et al., 2021)*, as well as manually designed coefficient determination strategies *(Li et al., 2018)*. These methods typically require iterative adjustments, consuming considerable time, and may not easily converge to the optimal solution. The H-infinity state feedback controller is a robust feedback controller *(Su, 2010)*. In the design, the robustness requirements of the system for uncertain parameters and disturbances can be transformed into the form of linear matrix inequalities (LMIs), which can be used as a constraint to efficiently solve the gain coefficient of optimal control law and achieve the robustness of the controller. In recent years, the application of H-infinity state feedback control in non-agricultural vehicles has been increasing, but its development in agricultural machinery has been relatively limited. Rath and Subudhi *(2022)* proposed a robust MPC control algorithm based on the H-infinity index, which improves the robustness of unmanned underwater vehicles to environmental disturbances while ensuring that their path-tracking control meets control constraints. *Legrand et al (2022)* designed a path-tracking controller for off-road vehicles based on H2/H-infinity control. It improved the robustness of the off-road vehicle path-tracking controller to uncertain parameters such as road slope, cornering stiffness, and road adhesion coefficient.

Gagliardy et al (2022) designed a path-tracking controller for autonomous vehicles during automatic following based on H-infinity state feedback control, which improved the robustness of autonomous vehicles to path curvature disturbance, front vehicle acceleration disturbance, and longitudinal speed uncertainty in a simulation environment. In agricultural machinery, *Fukumoto et al (2022)* applied H-infinity state feedback control to the arm length control mechanism in automatic spinach harvesters. In the path-tracking control of rice transplanters, the H-infinity state feedback control has not yet been applied and practiced. To this end, a curved path-tracking controller is designed for rice transplanters based on H-infinity state feedback control.

To improve the accuracy of curved path-tracking for transplanter headland turning, taking the tracking error model based on Two-DOF vehicle dynamics as the model, based on the H-infinity state feedback control, a curved path-tracking controller is designed. Finally, the control accuracy of the proposed controller is verified by using the YANMAR VP6E rice transplanter.

MATERIALS AND METHODS

Experimental materials

The experimental platform is the modified YANMAR VP6E rice transplanter shown in Fig. 1, and the basic parameters are shown in Table 1. The accelerator pedal and brake pedal of the transplanter are modified to be controlled by an electric push rod, and the speed of transplanter is controlled by a STM32 controller adjusting the electric push rod. The steering of the transplanter is controlled by a controller driving a DC motor-driven gear mechanism, thereby regulating the rotation of the steering wheel. The front wheel angle sensor measures the front wheel angle in real time, thereby achieving closed-loop control of the front wheel angle of the transplanter. The navigation equipment is the CHC CGI-610 centimeter-level integrated navigation system, configured to send data at a frequency of 10Hz according to the GPCHC data transmission protocol. During path-tracking, the STM32 controller first receives the pose of the transplanter sent by the integrated navigation, and then calculates the state error based on the actual rice transplanter pose and the expected path point input in advance. Finally, based on the state error matrix and the control law input in advance, the expected front wheel angle is calculated to achieve path-tracking of the rice transplanter.

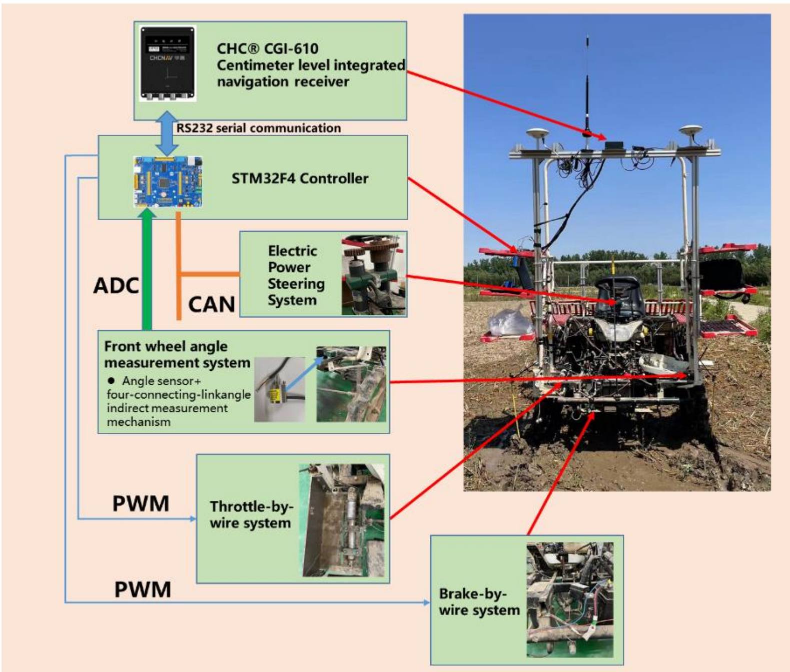

Fig. 1 - Modified YANMAR VP6E rice transplanter

Table 1

Basic vehicle parameters

Parameters	Values
Vehicle mass *m,* (kg)	496
Distance from the center of mass to the front axle *a,* (m)	0.65
Distance from the center of mass to the rear axle *b,* (m)	0.4
Moment of inertia around the z-axis I_z, (kg/m^2)	124
The maximum front wheel absolute angle δ_m / (°)	57

Tracking error model

A tracking error model based on Two-DOF vehicle dynamics is used to design the curved path-tracking controller of the rice transplanter. The tracking error model is shown in Fig. 2. According to two-DOF vehicle dynamic model, the tire slip angle formula, and the relationship between the front wheel angle and the front wheel sideslip angle, the state space equation of the tracking error model can be derived and simplified, as shown in Eq. (1) *(Hossain et al., 2022)*.

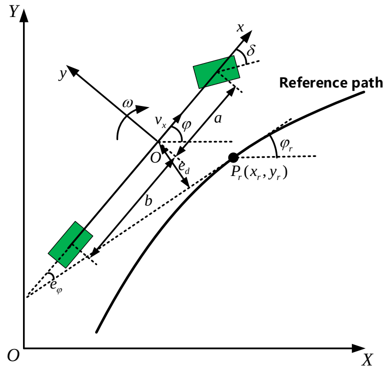

Fig. 2 - Tracking error model

$$\begin{cases} \dot{X} = AX + BU + CW \\ Y = DX \end{cases} \tag{1}$$

where:

$$A = \begin{bmatrix} 0 & 1 & 0 & 0 \\ 0 & -\dfrac{2C_{af} + 2C_{ar}}{mv_x} & \dfrac{2C_{af} + 2C_{ar}}{m} & -\dfrac{2aC_{af} - 2bC_{ar}}{mv_x} \\ 0 & 0 & 0 & 1 \\ 0 & -\dfrac{2aC_{af} - 2bC_{ar}}{I_z v_x} & \dfrac{2aC_{af} - 2bC_{ar}}{I_z} & -\dfrac{2a^2C_{af} + 2b^2C_{ar}}{I_z v_x} \end{bmatrix} \quad B = \begin{bmatrix} 0 \\ \dfrac{2C_{af}}{m} \\ 0 \\ \dfrac{2aC_{af}}{I_z} \end{bmatrix} \quad C = \begin{bmatrix} 0 \\ -\dfrac{2aC_{af} - 2bC_{ar}}{mv_x} - v_x \\ 0 \\ -\dfrac{2a^2C_{af} + 2b^2C_{ar}}{mv_x} \end{bmatrix}$$

$$X = \begin{bmatrix} e_d \\ \dot{e}_d \\ e_\varphi \\ \dot{e}_\varphi \end{bmatrix} \quad U = \delta \quad W = \dot{\varphi}_r$$

where:

m is the mass of rice transplanter; v_x is the longitudinal speed; I_z is the moment of inertia around the z-axis; a is the longitudinal distance between the center of mass and the front axle; b is the longitudinal distance between the center of mass and the rear axle; φ is the heading angle of rice transplanter; φ_r is the heading angle of reference path; δ is the front wheel steering angle; C_{af} is the cornering stiffness of front wheel; C_{ar} is the cornering stiffness of rear wheel; e_d is the lateral error between the center of mass and the nearest reference path point ahead; e_φ is the heading angle error between the center of mass and the nearest reference path point ahead, and D is the output matrix.

Controller design based on H-infinity state feedback control

When controlling the curved path-tracking, the controller designed based on the tracking error model of two-DOF vehicle dynamics is mainly affected by three factors: path curvature disturbance $W = \dot{\varphi}_r = \dfrac{v_x}{r}$, longitudinal speed uncertainty, and cornering stiffness uncertainty. The H-infinity state feedback controller is a robust feedback controller that can effectively enhance the robustness of the control system to path curvature disturbance and uncertain parameters.

Design principles of the controller

For the open-loop system described in Eq. (1) in the form of $\begin{cases} \dot{X} = AX + BU + CW \\ Y = DX \end{cases}$ *(Su, 2010)*, H-infinity state feedback control achieves asymptotic stability of the system by designing an optimal control law $U = KX$, making the disturbance term W having as little gain as possible on the output Y, that is, the infinity norm $\|T_{WY}(s)\|_{\infty}$ of the closed-loop transfer function $T_{WY}(s) = D[sI - (A+BK)]^{-1}C$ from W to Y is as small as possible, thus achieving system's robustness to disturbances. At the same time, if the problem of solving the optimal control law gain coefficient K mentioned above is transformed into a convex optimization problem containing LMIs, it can greatly simplify the solving process and improve the solving efficiency. When the parameters in matrices A, B and C are uncertain, the LMIs problem with uncertain parameters can be transformed into solving the LMIs problem corresponding to the upper and lower bounds of the uncertain parameters only based on the properties of convex function and amplification technique. In this way, it is ensured that the sensitivity of system to disturbances is reduced while the robustness of system to uncertain parameters is improved.

Lemma

To transform the solving of the gain coefficient of the control law into a convex optimization problem with LMIs, and to address issues related to parameter uncertainty and disturbances, the following lemma needs to be used *(Su, 2010)*:

Lemma 1 *(Su, 2010)*:

For a given constant $\gamma > 0$ and the system state equation $\begin{cases} \dot{X} = AX + CW \\ Y = DX \end{cases}$, the following two conditions are equivalent:

(1) The system is asymptotically stable with EE (Energy to Energy) gain $\Gamma_{ee} < \gamma$;

(2) There is a symmetric matrix $P > 0$, such that $\begin{bmatrix} A^T P + PA & PC & D \\ C^T P & -\gamma I & 0 \\ D^T & 0 & -\gamma I \end{bmatrix} < 0$

where X is the state quantity; W is the disturbance, and Y is the output.

Lemma 2 *(Boyd et al., 1994)*: When $f(x)$ is a convex function defined on a compact convex set Ω, $f(x) < 0, x \in \Omega \Leftrightarrow f(x) < 0, x \in \Omega_E$, where Ω_E represents the pole of the convex set.

Lemma 3 (Amplification technique) *(Boyd et al., 1994)*: For symmetric matrix Y, real matrices Γ and ψ with appropriate dimensions, if there is a matrix Λ satisfying $\Lambda^T \Lambda \le I$, then the inequality $Y + \Gamma\Lambda\psi + \psi^T \Lambda^T \Gamma^T < 0$ holds if and only if there is a constant $\varepsilon > 0$, such that $Y + \varepsilon\Gamma\Gamma^T + \varepsilon^{-1}\psi^T\psi < 0$.

Lemma 4 (Schur complement lemma) *(Boyd et al., 1994)*: $S_{22} < 0, \begin{bmatrix} S_{11} & S_{12} \\ S_{21} & S_{22} \end{bmatrix} < 0 \Leftrightarrow S_{11} - S_{12}S_{22}S_{21} < 0$.

Solving the gain coefficient of control law

For model (1), according to Lemma 1, the problem of reducing the output gain caused by path curvature disturbance can be transformed into a convex optimization problem with LMIs shown as Eq. (2). After solving Eq. (2) to obtain the matrix F and matrix G, the gain coefficient $K = FG^{-1}$ of the controller control law making system resistant to path curvature disturbance can be obtained first.

$$\min \gamma$$
$$s.t. \begin{bmatrix} (AG+BF)+(AG+BF)^T & C & GD \\ C^T & -\gamma I & 0 \\ (GD)^T & 0 & -\gamma I \end{bmatrix} < 0 \tag{2}$$
$$P > 0$$

Proof: Multiply the left and right ends of the first LMI in Eq. (2) by symmetric matrix $diag(P, E, E)$, it is obtained that:

$$\begin{bmatrix} P(AG+BF)P+P(AG+BF)^T P & PC & PGD \\ C^T P & -\gamma I & 0 \\ (GD)^T P & 0 & -\gamma I \end{bmatrix} < 0 \tag{3}$$

Let $K = FG^{-1}$, $G = P^{-1}$, substituting into Eq.(3), it can be obtained that

$$\begin{bmatrix} P(A+BK)+(A+BK)^T P & PC & D \\ C^T P & -\gamma I & 0 \\ D^T & 0 & -\gamma I \end{bmatrix} < 0 \tag{4}$$

Eq. (4) is the form that satisfies Lemma 1, thus proved.

At this point, the problem solved by Eq. (2) is only to reduce the interference of path curvature disturbance on the tracking performance of the controller.

The controller also needs to consider robustness to uncertain parameters. Based on Eq. (2), the robustness of the controller to longitudinal speed is introduced. The longitudinal speed of the vehicle exists in matrices *A*, *B* and *C*, and the linear matrix in Eq. (2) can be regarded as a function of v_x. It is known that the set of v_x is a convex set, and the left linear matrix of the first LMI in Eq. (2) is a convex function. Therefore, substituting the poles of the convex set of v_x into Eq. (2), Eq. (5) can be obtained as follow:

$$\begin{gathered} \min \gamma \\ s.t. \begin{bmatrix} sys(A_i G + B_i F) & C_i & GD \\ C_i^T & -I & 0 \\ (GD)^T & 0 & -\gamma I \end{bmatrix} < 0 \quad i = 1,2 \ldots n \\ G > 0 \end{gathered} \tag{5}$$

where, *n* is the number of poles on the convex set of v_x; *A*, *B* and *C* are the matrices corresponding to v_x at the *i* th pole of the convex set of v_x.

Combined with Lemma 2, it can be inferred that the gain coefficient $K = FG^{-1}$ of control law obtained by solving Eq. (5) can make the controller robust to path curvature disturbance and longitudinal speed.

To introduce the uncertainty term of cornering stiffness into the tracking error model based on Two-DOF vehicle dynamics, uncertainty terms ΔA and ΔB are introduced into Eq. (1). Thus, Eq. (1) is transformed into the form of the parameter perturbation model *(Su 2010)*, as shown in Eq. (6).

$$\begin{cases} \dot{X} = (A+\Delta A)X + (B+\Delta B)U + (C+\Delta C)W \\ Y = DX \end{cases} \tag{6}$$

Where, $\Delta A = \begin{bmatrix} 0 & 1 & 0 & 0 \\ 0 & -\dfrac{2\tilde{C}_{af}+2\tilde{C}_{ar}}{mv_x} & \dfrac{2\tilde{C}_{af}+2\tilde{C}_{ar}}{m} & -\dfrac{2a\tilde{C}_{af}-2b\tilde{C}_{ar}}{mv_x} \\ 0 & 0 & 0 & 1 \\ 0 & -\dfrac{2a\tilde{C}_{af}-2b\tilde{C}_{ar}}{I_z v_x} & \dfrac{2a\tilde{C}_{af}-2b\tilde{C}_{ar}}{I_z} & -\dfrac{2a^2\tilde{C}_{af}+2b^2\tilde{C}_{ar}}{I_z v_x} \end{bmatrix}$ $\Delta B = \begin{bmatrix} 0 \\ \dfrac{2\tilde{C}_{af}}{m} \\ 0 \\ \dfrac{2a\tilde{C}_{af}}{I_z} \end{bmatrix}$

$\Delta C = \begin{bmatrix} 0 \\ -\dfrac{2a\bar{C}_{af}-2b\bar{C}_{ar}}{mv_x} - v_x \\ 0 \\ -\dfrac{2a^2\bar{C}_{af}+2b^2\bar{C}_{ar}}{mv_x} \end{bmatrix}$ $\tilde{C}_{af} = \lambda \bar{C}_{af}$ $\tilde{C}_{ar} = \lambda \bar{C}_{ar}$ $\bar{C}_{af} = \dfrac{C_{af\max} - C_{af\min}}{2}$ $\bar{C}_{ar} = \dfrac{C_{ar\max} - C_{ar\min}}{2}$ $|\lambda| \le 1$

Then, according to the method of handling parameter perturbation models *(Su 2010)*, ΔA and ΔB can be represented in the following form:

$$[\Delta A \quad \Delta B \quad \Delta C] = H\Lambda[E_1 \quad E_2 \quad E_3] \tag{7}$$

where $\Lambda = diag(\lambda, \lambda, \lambda)$

$$H=\begin{bmatrix}0&1&0&0\\0&0&0&1\end{bmatrix}^T \quad E_1=\begin{bmatrix}0 & -\dfrac{2\bar{C}_{af}+2\bar{C}_{ar}}{mv_x} & \dfrac{2\bar{C}_{af}+2\bar{C}_{ar}}{m} & -\dfrac{2a\bar{C}_{af}-2b\bar{C}_{ar}}{mv_x}\\ 0 & -\dfrac{2a\bar{C}_{af}-2b\bar{C}_{ar}}{I_z v_x} & \dfrac{2a\bar{C}_{af}-2b\bar{C}_{ar}}{I_z} & -\dfrac{2a^2\bar{C}_{af}+2b^2\bar{C}_{ar}}{I_z v_x}\end{bmatrix} \quad E_2=\begin{bmatrix}\dfrac{2\bar{C}_{af}}{m}\\ \dfrac{2a\bar{C}_{af}}{I_z}\end{bmatrix}$$

$$E_3=\begin{bmatrix}-\dfrac{2a\bar{C}_{af}-2b\bar{C}_{ar}}{mv_x}-v_x\\ -\dfrac{2a^2\bar{C}_{af}+2b^2\bar{C}_{ar}}{mv_x}\end{bmatrix}$$

Finally, combined with Eqs. (5), (6) and (7) and the amplification technique *(Su, 2010)*, the problem of solving the gain coefficient of the control law for the curved path-tracking controller of a rice transplanter based on H-infinity state feedback control, which is robust to uncertain parameters (longitudinal speed and cornering stiffness) and path curvature disturbance, can be transformed into a convex optimization problem with LMIs as follows:

$$\min \gamma$$
$$s.t.\begin{bmatrix} sys\ (A_iG+B_iF) & GC_i & G & (E_{1i}R+E_2F)^T & GH\\ * & -\gamma I & 0 & E_{3i}^T & 0\\ * & * & -\gamma I & 0 & 0\\ * & * & * & -\varepsilon_i I & 0\\ * & * & * & * & -\varepsilon_i^{-1}I\end{bmatrix}<0 \quad i=1,2\ldots n \tag{8}$$
$$P>0$$
$$P=P^T$$

where:

$sys(\bullet)=\bullet+\bullet^T$; n is the number of poles on the convex set of v_x; A_i, B_i, C_i, E_{1i} and E_{3i} are the matrices corresponding to v_x at the i-th pole of the convex set of v_x; $*$ is the symmetric element in the symmetric matrix.

Proof: first, there is:

$$\begin{aligned}&sys(A_iP+\Delta A_iP+B_iKP+\Delta BKP)\\ &=sys(A_iP+H\Lambda E_{1i}P+B_iKP+H\Lambda E_2KP)\\ &=sys(A_iP+B_iKP)+sys(H\Lambda(E_{1i}+E_2K)P)\end{aligned} \tag{9}$$

Combined Lemma 3 with Lemma 4, it is obtained that

$$\begin{aligned}&\begin{bmatrix} sys\ (PA_i+P\Delta A_i+PB_iK+P\Delta BK) & P(C_i+\Delta C_i) & D\\ (C+\Delta C)^TP & -\gamma I & 0\\ D^T & 0 & -\gamma I\end{bmatrix}\\
&=\begin{bmatrix} sys\ (PA_i+PB_iK) & PC_i & D\\ C_i^TP & -\gamma I & 0\\ D^T & 0 & -\gamma I\end{bmatrix}+sys\left\{\begin{bmatrix}PH\\0\\0\end{bmatrix}\Lambda\begin{bmatrix}E_{1i}+E_2K & E_{3i} & 0\end{bmatrix}\right\}\\
&<\begin{bmatrix} sys\ (PA_i+PB_iK) & PC_i & D\\ C_i^TP & -\gamma I & 0\\ D^T & 0 & -\gamma I\end{bmatrix}+\varepsilon_i\begin{bmatrix}PH\\0\\0\end{bmatrix}\begin{bmatrix}PH\\0\\0\end{bmatrix}^T+\varepsilon_i^{-1}\begin{bmatrix}E_{1i}+E_2K & E_{3i} & 0\end{bmatrix}^T\begin{bmatrix}E_{1i}+E_2K & E_{3i} & 0\end{bmatrix}\\
&=\begin{bmatrix} sys\ (PA_i+PB_iK) & PC_i & D & (E_{1i}+E_2K)^T & PH\\ * & -\gamma I & 0 & E_{3i}^T & 0\\ * & * & -\gamma I & 0 & 0\\ * & * & * & -\varepsilon_i I & 0\\ * & * & * & * & -\varepsilon_i^{-1}I\end{bmatrix}\end{aligned} \tag{10}$$

Multiplying $diag\ (P^{-1}, I, I, I, I)$ on both sides of the above equation, it is obtained that:

$$\begin{bmatrix} sys\ (A_i P^{-1} + B_i K P^{-1}) & C_i & P^{-1}D & (E_{1i}P^{-1} + E_2 K P^{-1})^T & P^{-1}H \\ * & -\gamma I & 0 & E_{3i}^T & 0 \\ * & * & -\gamma I & 0 & 0 \\ * & * & * & -\varepsilon_i I & 0 \\ * & * & * & * & -\varepsilon_i^{-1} I \end{bmatrix} \tag{11}$$

Let $F = KP^{-1}$ and $G = P^{-1}$, the above formula can be transformed as follows:

$$\begin{bmatrix} sys\ (A_i G + B_i F) & C_i & GD & (E_{1i}G + E_2 F)^T & GH \\ * & -\gamma I & 0 & E_{3i}^T & 0 \\ * & * & -\gamma I & 0 & 0 \\ * & * & * & -\varepsilon_i I & 0 \\ * & * & * & * & -\varepsilon_i^{-1} I \end{bmatrix} \tag{12}$$

Thus, Eq. (8) is proved.

Finally, using the LMI toolkit in Matlab to solve the convex optimization problem shown in Eq. (8), the matrix F and G can be obtained. Then the gain coefficient of the control law for the curved path-tracking controller of a rice transplanter based on H-infinity state feedback control, which is robust to uncertain parameters (longitudinal speed and cornering stiffness) and path curvature disturbance, can be obtained. The control law is $U = KX = FG^{-1}X$.

RESULTS AND ANALYSIS

Reference path and initial pose of the rice transplanter

According to the relationship between working spacing and turning radius, the headland turning mode of the rice transplanter should be *T*-turn, which is composed of 1/4 arc and straight-line *(Trendafilov and Tihanov, 2022)*. Combined with the actual situation of the rice transplanter headland turning, a 1/4 arc with a radius of 2 m is selected as the reference path to evaluate the curved path-tracking effect of the path-tracking controller.

At the beginning of the experiment, the initial heading angle of the transplanter is adjusted to 90 ° and the initial front wheel angle to 0° in the geodetic coordinate system. The controller first obtains the starting position (x_0, y_0) of the transplanter, and then use $(x_0 + 0.02\ \text{m},\ \ y_0 + 0.06\ \text{m})$ as the starting point of the reference path to make a 1/4 arc with a radius of 2 m clockwise. This serves as the reference path for the transplanter curved path-tracking, then discretizes the reference path into 40 reference path points at an interval of $\Delta x = 0.05\ \text{m}$.

Determination of system model parameters and controller parameters

To calculate the control law gain coefficient of the controller, it is necessary to determine all parameters in Eq. (8). To obtain the range of longitudinal speed variation, the PID algorithm is used to control the longitudinal speed of the rice transplanter to maintain around 0.7 m/s, then let the transplanter turn along a 1/4 arc with a radius of 2 m, and obtain the speed measured by the integrated navigation. The variation curve of the longitudinal speed is shown in Fig. 3. From Fig. 3, it can be seen that the longitudinal speed of the rice transplanter is basically maintained between 0.5 m/s and 0.8 m/s. Therefore, the nominal longitudinal speed v_x during the path-tracking process is selected as 0.7 m/s, and the upper bound $v_{x_{\max}}$ and lower bound $v_{x_{\min}}$ of the longitudinal speed are 0.5 m/s and 0.8 m/s, respectively.

To obtain the nominal value and range of cornering stiffness, based on the identification results of the cornering stiffness of the transplanter in reference *(Li et al., 2020)* and combined with magic formulas, the cornering stiffness of the transplanter tire used in the experiment is estimated. The upper and lower limits of the cornering stiffness of the front and rear tires are obtained as 625 N/rad, 250 N/rad, 776 N/rad and 258N/rad, respectively. The nominal cornering stiffness C_{af} of the front tire was 400 N/rad, and the nominal cornering stiffness C_{ar} of the rear tire was 517 N/rad.

As the output of the H-infinity state feedback controller increases, the conservatism of the controller will improve, leading to a decrease in control accuracy. Thus, the designed H-infinity state feedback controller only controls the lateral error and heading angle error, and does not control their rate of change. The output matrix $D = diag\ (1, 0, 1, 0)$ is selected.

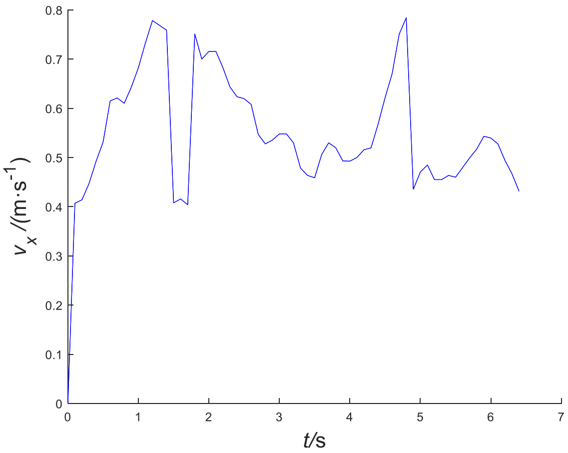

Fig. 1 - Longitudinal speed variation curve

To acquire the LQR controller (which has relatively good tracking performance) to be compared with the H-infinity state feedback controller, and to verify the improvement effect of the H-infinity state feedback controller on the curved path-tracking accuracy of the transplanter, leveraging the method described in reference *(Xu et al., 2022)* for calculating the gain coefficients of the LQR controller control law, based on experience, the parameter of the control input weight of the LQR controller is selected to be 0.1, based on the parameters in Table 1 and the nominal longitudinal speed and nominal cornering stiffness, the weight parameters of the state error weight matrix Q in the calculation of the LQR controller control law gain coefficient are exhaustively tested from 1 to 100 with 4 intervals through CarSim-Simulink co-simulation, the state error weight matrix $Q = diag\ (49,1,25,1)$ that minimizes the mean absolute lateral error is obtained.

Simulation experiments and discussions

To verify the impact of path curvature disturbance and parameter uncertainty on the tracking accuracy of the controller path, and to verify the effectiveness of the H-infinity state feedback controller, the LQR controller, feedforward LQR controller, and H-infinity state feedback controller in tracking the path described in section 3.2 are compared through CarSim-Simulink co-simulation.

The control laws of the H-infinity state feedback controller and the LQR controller are as follows:

$$U = KX \tag{13}$$

The control law of the feedforward LQR controller (obtained according to the method in reference *(Xu and Liu, 2022)* is as follows:

$$\begin{aligned} U = KX + \dot{\varphi}_r [a + b - bK_3 + \\ \frac{m v_x^{\ 2}}{a+b}(-\frac{b}{2C_{af}} - \frac{a}{2C_{ar}}K_3 + \frac{a}{2C_{ar}})] \end{aligned} \tag{14}$$

where, K_3 is the third element in the matrix K.

The simulation time step is set to 1ms, and the parameters of the transplanter are set as shown in Table 1. The initial state is the same as described in Section 3.2. To make the simulation effect closer to the actual application effect in paddy fields, the function of longitudinal speed variation with time is approximately fitted based on the actual longitudinal speed of the rice transplanter when turning in the paddy field obtained in Section 3.3, as shown in Eq. (15).

$$v_x = 0.6 + 0.2\sin(\frac{\pi}{2}t - \frac{\pi}{4})\ (\mathrm{m/s}) \tag{15}$$

During the simulation experiment, the above function is input into the simulation model to change the longitudinal speed of the transplanter in real time, so that the influence of the complex environment of paddy fields on the longitudinal speed of the transplanter is simulated. The corresponding relationship between cornering stiffness and load in Carsim is estimated and designed based on the nominal cornering stiffness obtained in section 3.3 and the magic formula. In the simulation process, taking the rice transplanter controlled by the LQR controller as an example, the cornering stiffness change curve is output, as shown in Fig. 4 (d).

During the experiment (so as the field test), the tracking error is calculated by the method described in reference *(Xu et al., 2022)*. Finally, the simulation results of path-tracking are shown in Fig. 4, and the simulation data statistics are shown in Table 2.

The simulation results are analyzed according to Fig. 4 and Table 2. In terms of lateral error, the H-infinity state feedback controller considering path curvature disturbance and parameter uncertainty, has the best tracking performance, followed by the feedforward LQR controller, and the LQR controller is the worst. From the perspective of heading angle error, the performance of the H-infinity state feedback controller is relatively poor compared to the other two controllers. The overall tracking performance of the three controllers based on the proximity between the actual path and the reference path of the rice transplanter is evaluated, the H-infinity state feedback controller has the best tracking performance, followed by the feedforward LQR controller, and the LQR controller is the worst.

Figs. 3 and 4 (d) can represent the changes in uncertain parameters during the simulation process. The longitudinal speed is generally between 0.5 m/s and 0.8 m/s; the cornering stiffness of the front tire is generally between 200 N/rad and 600 N/rad, and the cornering stiffness of the rear tire is generally between 300 N/rad and 800 N/rad. The path curvature disturbance in this experiment is approximately $W = \dot{\varphi}_r = \frac{v_x}{r} = \frac{0.7}{2} = 0.35\ (s^{-1})$. The above experimental results show that when there are uncertain parameters and path curvature disturbance, the LQR controller has relatively poor path-tracking performance due to not considering the above two issues. After incorporating feedforward control, improvements are made to address the issue of path curvature disturbance, resulting in improved path-tracking performance. For the H-infinity state feedback controller, due to its consideration of robustness to path curvature disturbance and uncertain parameters, it achieves the best path-tracking performance.

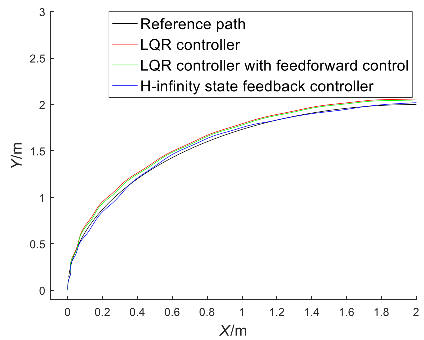

(a) Actual path of the rice transplanter

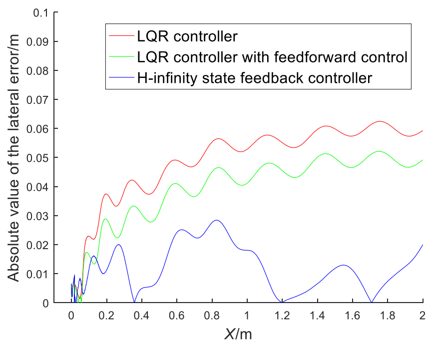

(b) Absolute value curve of the lateral error

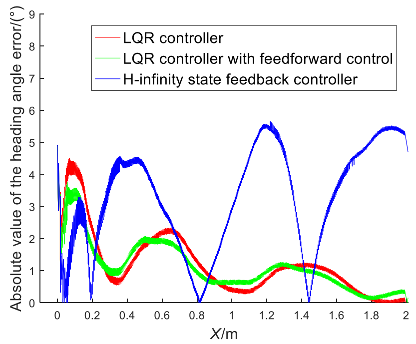

(c) Absolute value curve of the heading angle error

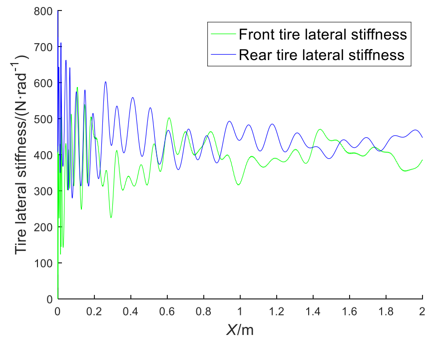

(d) Variation curve of the cornering stiffness (under LQR controller control)

Fig. 4 - Simulation test results

Table 2

Data statistics of the simulation results

Controllers	Lateral error			Heading angle error		
	Mean absolute value / m	Maximum absolute value / m	Absolute value less than 0.04 m / (%)	Mean absolute value / (°)	Maximum absolute value / (°)	Absolute value less than 5°/ (%)
LQR controller	0.036	0.062	48	1.98	4.94	100
Feedforward LQR controller	0.029	0.052	60	1.81	4.94	100
H-infinity State Feedback Controller	0.011	0.028	100	2.97	5.65	95

Field experiments and discussions

To verify the actual effectiveness of the controller, the feedforward LQR controller and H-infinity state feedback controller will be used for actual vehicle control. During the path-tracking process of the rice transplanter, the PID algorithm is used to maintain the longitudinal speed v_x around 0.7 m/s. The experimental scenario is shown in Fig. 5.

(a) Test site (b) Path-tracking test of the transplanter headland turning

Fig. 5 - Experimental scenario of curved path-tracking for the rice transplanter on the field

After the experiment, the actual path and absolute lateral error variation curves of the rice transplanter under the feedforward LQR controller and the H-infinity state feedback controller, as well as the absolute heading angle error variation curve, can be obtained as shown in Fig. 6. The specific statistical data is shown in Table 3.

As shown in Fig. 6, the actual path of the rice transplanter under the control of the H-infinity state feedback controller is closer to the expected path than the actual path under the feedforward LQR controller. The lateral error of the H-infinity state feedback controller is generally smaller than that of the feedforward LQR controller, but the heading angle error is larger than that of the feedforward LQR controller.

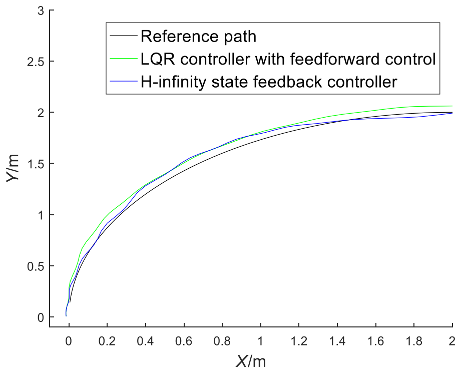

(a) Actual path of the rice transplanter

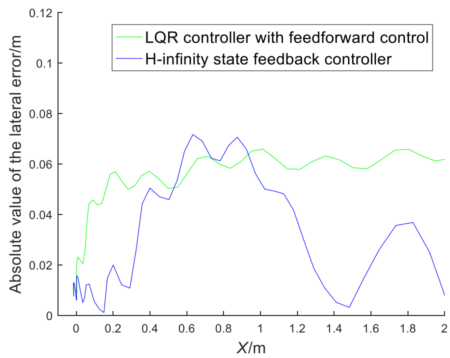

(b) Absolute value curve of the lateral error

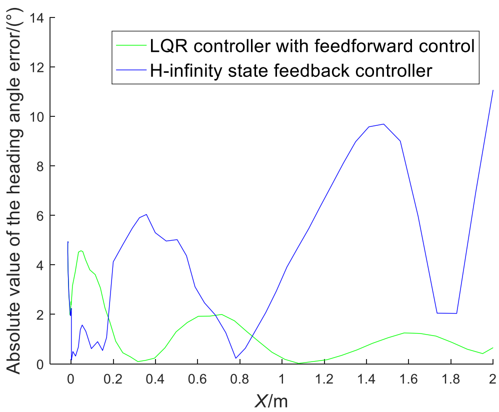

(c) Absolute value curve of the heading angle error

Fig. 6 - Field test results

Table 3

Comparison of the tracking error

Controllers	Lateral error				Heading angle error			
	Mean absolute value /m	Maximum absolute value / m	Minimum absolute value / m	Absolute value less than 0.04m / (%)	Mean absolute value / (°)	Maximum absolute value / (°)	Minimum absolute value / (°)	Absolute value less than 5 °/ (%)
Feedforward LQR controller	0.045	0.066	0.008	29	1.93	4.93	0.09	100
H-infinity State Feedback Controller	0.029	0.072	0.003	64	3.69	10.98	0.16	72

According to Table 3, the absolute lateral error under the H-infinity state feedback controller is reduced by 36% compared to the feedforward LQR controller, and the percentage of absolute lateral error less than 0.04 m is increased by 121%. However, for the absolute heading angle error, the mean value under the feedforward LQR controller is reduced by 48% compared to that under the H-infinity state feedback controller, and the percentage of error less than 5 ° under the feedforward LQR controller is increased by 39% compared to the H-infinity state feedback controller.

In summary, the control accuracy of the H-infinity state feedback controller for curved path-tracking of unmanned rice transplanters meets practical requirements and can be applied to headland turning control of unmanned rice transplanters. The actual path of the rice transplanter under its control is closer to the expected path compared to the LQR controller with feedforward control. The lateral error is reduced and the heading angle error is improved. Overall, the H-infinity state feedback controller has better path-tracking performance and stronger robustness.

CONCLUSIONS

(1) To improve the accuracy of curved path-tracking when unmanned rice transplanters turns at the headland, a design method for a curved path-tracking controller of a rice transplanter based on H-infinity state feedback control is proposed. This method transforms the robustness requirements of the controller to uncertain parameters (longitudinal speed, cornering stiffness) and disturbance (path curvature disturbance) into the form of LMIs, and uses it as a constraint to solve the gain coefficient of optimal control law, achieving the robustness of the controller to uncertain parameters and disturbance.

(2) The simulation test results show that when the rice transplanter tracks the path of a 1/4 arc with a radius of 2 m, and the longitudinal speed and cornering stiffness fluctuate, the path-tracking performance of LQR controller is relatively poor due to not considering path curvature disturbance and parameter uncertainty. After incorporating feedforward control, improvements are made to address the issue of path curvature disturbance, resulting in improved path-tracking performance. For the H-infinity state feedback controller, due to its consideration of robustness to path curvature disturbance and uncertain parameters, it can achieve better path-tracking performance than the LQR controller and the feedforward LQR controller.

(3) The field test results show that when the rice transplanter tracks the path of a 1/4 arc with a radius of 2 m, the mean absolute values of lateral error and heading angle error under the H-infinity state feedback controller are 0.029 m and 3.69°, respectively. The maximum absolute lateral error is 0.072 m, and the absolute lateral errors less than 0.04 m account for 64%. Compared with the feedforward LQR controller, the mean absolute lateral error is reduced by 36%. It has been verified that the proposed path-tracking algorithm meets the accuracy and robustness requirements of path-tracking when the transplanter turns at the headland.

ACKNOWLEDGEMENTS

The work was supported by the National Natural Science Foundation of China (52172396).

REFERENCES

[1] Boyd, S., Ghaoui, L.E., Feron, E., Balakrishnan, V. (1994). Linear Matrix In-equalities in Systems and Control Theory. SIAM Studies in *Applied Mathematics*. https://epubs.siam.org/doi/book/10.1137/1.9781611970777

[2] Chi, R.J., Xiong, Z.X., Jiang, L.T., Ma, Y.Q. and Huang, X.L., Zhu, X.L. (2022). Path-tracking control algorithm of transplanter based on model prediction (基于模型预测的插秧机路径跟踪控制算法). *Transactions of the Chinese Society for Agricultural Machinery*, Vol. 53(11), pp. 22-30, 99. (in Chinese)

[3] Dekhterman, S. R., Cichon, M. T., Norris, W. R., Nottage, D., Soylemezoglu, A. (2024). Hierarchical rule-base reduction fuzzy control for constant velocity path-tracking of a differential steer vehicle. *Journal of Field Robotics*. Vol. 41, pp. 718-734. https://doi.org/10.1002/rob.22287

[4] Fukumoto, T., Chida, Y., Tanemura, M. (2022). Improved tracking performance by H∞ control for an automatic spinach harvester. *IFAC-Papers OnLine,* Vol. 55(25), pp. 265-270. https://doi.org/10.1016/j.ifacol.2022.09.357

[5] Gagliardi, G., Casavola, A., Toscano, S. (2022). Linear Parameter Varying Control Strategies for Combined Longitudinal and Lateral Dynamics of Autonomous Vehicles. *2022 European Control Conference (ECC), (London, United Kingdom)*. Vol. 2022, pp.181-186. https://doi.org/10.23919/ECC55457.2022.9838177

[6] Gang, M., Kim, H.-J., Jeon, C.-W., Yun, C. (2022). Design and Testing of Headland Turning Algorithms Based on Transition Distance Prediction for Autonomous Rice Transplanter. *Journal of the ASABE,* Vol. 65(6), pp. 1277-1291. Doi: 10.13031/ja.14952

[7] Gökçe, B., Koca, Y. B., Aslan, Y., Gökçe, C. O. (2021). Particle swarm optimization-based optimal PID control of an agricultural mobile robot. *Comptes rendus de l'Acade'mie bulgare des Sciences*. Vol. 74(4), pp. 568-575. DOI: 10.7546/CRABS.2021.04.12

[8] Gong, J.W., Jiang, Y., Xu, W. (2014). Model Predictive Control for Self-driving Vehicles. Beijing: Beijng institute of technology Press. (in Chinese)

[9] He, J., Hu, L., Wang, P., Liu, Y.X., Man, Z.X., Tu, T.P., Yang, L.N., Li, Y.Y., Yi, Y.L., Li, W.C., Luo, X.W. (2022). Path-tracking control method and performance test based on agricultural machinery pose correction. *Computers and Electronics in Agriculture*, Vol. 200, pp. 107185. https://doi.org/10.1016/j.compag.2022.107185

[10] Hossain, T., Habibullah, H., Isiam, R. (2022). Steering and Speed Control System Design for Autonomous Vehicles by Developing an Optimal Hybrid Controller to Track Reference Trajectory. *Machines*, Vol. 10, pp. 420. https://doi.org/10.3390/machines10060420

[11] Ji, X., Ding, S.H., Wei, X.H., Cui, B.B. (2023). Path-tracking of unmanned agricultural tractors based on a novel adaptive second-order sliding mode control. *Joumal of the Franklin Institute,* Vol. 360(8), pp. 5881-5831. https://doi.org/10.1016/j.jfranklin.2023.03.053

[12] Kim, S., Jang, M., La, H., Oh, K. (2023). Development of a Particle Filter-Based Path-tracking Algorithm of Autonomous Trucks with a Single Steering and Driving Module Using a Monocular Camera. *Sensors,* Vol. 23, pp. 3650. https://doi.org/10.3390/s23073650

[13] Legrand, R., Claveau, F., Chevrel, P., Rancinangue, B., Dollet, A. (2022). H2/H∞ robust lateral control of an off-road two-steering-axle vehicle on slippery sloping soils. *IFAC-Papers OnLine*, Vol. 55(25), pp. 187-192. https://doi.org/10.1016/j.ifacol.2022.09.345

[14] Li, G., Wang, Y., Guo, L.F., Tong, J.H., He, Y. (2018). Improved pure pursuit algorithm for rice transplanter path-tracking (插秧机导航路径跟踪改进纯追踪算法). *Transactions of the Chinese Society for Agricultural Machinery,* Vol. 49(05), pp. 21-26. (in Chinese)

[15] Li, Y.B., Li, H., Guo, X.N. (2020). Online parameter identification of rice transplanter model based on IPSO-EKF algorithm. *INMATEH - Agricultural Engineering*, Vol. 61(2), pp. 25-34. https://doi.org/10.35633/inmateh-61-03

[16] Li, Y.M., Wu, T., Xiao, Y.F., Gong, L., Liu, C.L. (2023). Path planning in continuous adjacent farmlands and robust path-tracking control of a rice-seeding robot in paddy field. *Computers and Electronics in Agriculture,* Vol. 210, 107900. https://doi.org/10.1016/j.compag.2023.107900

[17] Oh, K., Seo, J. (2023). Development of a Sliding-Mode-Control-Based Path-Tracking Algorithm with Model-Free Adaptive Feedback Action for Autonomous Vehicles. *Sensors*, Vol. 23, pp. 405. https://doi.org/10.3390/s23010405

[18] Rath, B.N., Subudhi, B. (2022). A robust model predictive path following controller for an Autonomous Underwater Vehicle. *Ocean Engineering*, Vol. 244, pp. 110265. https://doi.org/10.1016/j.oceaneng.2021.110265

[19] Shojaei, K., Taghavifar, H. (2022). Input-output feedback linearization control of a tractor with n-trailers mechanism considering the path curvature. Proceedings of the Institution of Mechanical Engineers. *Part C: Journal of Mechanical Engineering Science,* Vol. 236(17), pp. 9700-9715. https://doi.org/10.1177/09544062221088236

[20] Simonelli, R., Höffmann, M., Patel, S., Büskens, C. (2023). Optimal Path-tracking: Benchmarking an NMPC for a Wide-Span Autonomous Agricultural Machine. *2023 European Control Conference (ECC)*, *(Bucharest, Romania).* Vol. 2023, pp.1-7. https://doi.org/10.23919/ECC57647.2023.10178268

[21] Su, H. Y. (2010). Basic Theory of Robust control. Beijing: Science Press. (in Chinese)

[22] Taghia, J., Wang, X., Lam, S., Katupitiya, V. (2017). A sliding mode controller with a nonlinear disturbance observer for a farm vehicle operating in the presence of wheel slip. *Robot,* Vol. 41(1), pp. 71-88. https://doi.org/10.1007/s10514-015-9530-4

[23] Tang, X.T., Tao, J.F., Li, Z.T., Li, Y.M., Liu, C.L. (2018). Fuzzy control optimization method for stability of path-tracking system of automatic transplanter (自动导航插秧机路径跟踪系统稳定性模糊控制优化方法). *Transactions of the Chinese Society for Agricultural Machinery,* Vol. 49(01), pp. 29-34. (in Chinese)

[24] Trendafilov, K., Tihanov, G. (2022). Comparative Analysis of the Headland Width when Making T-turns by a Mounted Machine-Tractor Unit on an Irregularly-Shaped Field. *INMATEH-Agricultural Engineering,* Vol. 67(2), pp. 221-232. https://doi.org/10.35633/inmateh-67-22

[25] Xu, M.Z., Liu, Q.H. (2022). Design and simulation of intelligent vehicle trajectory tracking control algorithm based on LQR and PID (基于 LQR 和 PID 的智能车轨迹跟踪控制算法设计与仿真). *Journal of Taiyuan University of Technology,* Vol. 53(5), pp. 877-885. (in Chinese)

[26] Yang, Y., Li, Y.K., Wen, X., Zhang, G., Ma, Q.L., Cheng, S.K., Qi, J., Xu, L.Y., Chen, L.Q. (2022). An optimal goal point determination algorithm for automatic navigation of agricultural machinery: Improving the tracking accuracy of the Pure Pursuit algorithm. *Computers and Electronics in Agriculture,* Vol. 194, pp. 106760. https://doi.org/10.1016/j.compag.2022.106760